BILINGUAL PUBLISHING CO.
Pioneer of Global Academics Since 1984

Journal of Metallic Material Research
https://ojs.bilpublishing.com/index.php/jmmr

ARTICLE

Structure, Adhesion Strength and Corrosion Resistance of Vacuum Arc Multi-Period NbN/Cu Coatings

H.O. Postelnyk[1*] O.V. Sobol'[1] O. Chocholaty[2] G.I. Zelenskaya[1]

1. Kharkiv Polytechnic Institute, National Technical University, Kharkiv, 61002, Ukraine
2. University of West Bohemia, Univerzitní 2732/8, 301 00 Pilsen, Czech Republic

ARTICLE INFO

Article history
Received: 1 November 2019
Accepted: 14 November 2019
Published Online: 31 March 2020

Keywords:
Vacuum Arc method
NbN/Cu
Phase composition
Adhesion strength
Impedance spectroscopy
Polarization resistance

ABSTRACT

The influence of deposition modes on the phase-structural state, corrosion resistance, and adhesive strength of vacuum-arc multi-period NbN/Cu coatings is studied. It was found that in thin layers (about 8 nm, in a constant rotation mode), regardless of the change in the pressure of the nitrogen atmosphere, a metastable δ - NbN phase forms (cubic crystal lattice of the NaCl type). At a layer thickness of ~ 40 nm or more, a phase composition changes from the metastable δ - NbN to the equilibrium ε - NbN phase with a hexagonal crystal lattice. In the presence of the ε - NbN phase in the niobium nitride layers, the highest adhesive strength is achieved with a value of LC5 = 96.5 N. Corrosion resistance tests have shown that for all the studied samples the corrosion process has mainly an anodic reaction. The highest corrosion resistance was shown by coatings obtained at a pressure of $7 \cdot 10^{-4}$ Torr, with the smallest bias potential of -50 V and the smallest layer thickness; with a thickness of such a coating of about 10 microns, its service life in the environment of the formation of chloride ions is about a year.

1. Introduction

Niobium nitride (NbN) has a high melting point (about 2600 K), which is determined by the high binding energy (14.81 eV) [1]. NbN-based coatings have high functional characteristics (high hardness, wear resistance [2] and oxidation resistance [3], etc.), and also have a high critical temperature of superconductivity (Tc ≈ 16 K) [4]. There are several phases in the Nb-N system: β, δ, ε, γ, δ′, and η [5], which allows one to create different phase-structural states of coatings from niobium nitrides. Moreover, as is known, for nonequilibrium formation conditions (using vacuum-arc methods) for transition metal mononitrides, modifications with the structural type of NaCl are most often stabilized [6,7].

It is known that the properties of thin MeN films can be improved by adding a second "immiscible" metal (where Me is a transition metal) [8]. As an immiscible metal, Cu and Ag are used. In such a combination (MeCu and MeAg) materials have a good prospect for use as coatings in medical technology. Therefore, it is very important to know the adhesive strength and corrosion resistance of such coatings, which this work is devoted to [9].

The second important goal of this work was to establish the relationship of the deposition parameters with the phase-structural state and properties. This is the basis of structural engineering [10] and allows one to achieve the

**Corresponding Author:*
H.O. Postelnyk,
Kharkiv Polytechnic Institute, National Technical University, Kyrpychov Str., Kharkiv, 61002, Ukraine;
Email: annapostelnik@mail.ru

 DOI: https://doi.org/10.30564/jmmr.v3i1.1364

necessary properties by modeling the structure.

2. Material and Methods

The coatings were deposited on AISI 321 austenitic steel by the vacuum-arc method at the "Bulat-6" installation with various technological deposition conditions, the modes of which are given in Table 1.

Table 1. Technological parameters of deposition of NbN/Cu coatings

Series	PN, Torr	Ub, V	The condition for obtaining	Layer Thickness
1	$7 \cdot 10^{-4}$	-50	constant rotation	of about 8 nm
2	$3 \cdot 10^{-3}$	-50		
3	$7 \cdot 10^{-4}$	-50	20 s interval	40 nm
4	$7 \cdot 10^{-4}$	-200		
5	$3 \cdot 10^{-3}$	-100	120 s – Cu 300 s – Nb	240 nm – Cu 600 nm – Nb

Working gas pressure (PN) during coating deposition was 7·10-4 or 3·10-3 Torr; the bias potential supplied to the substrate varied from -50 to -200 V. The deposition was carried out from 2 sources (Nb and Cu) in the regimes with a constant rotation speed (rotation speed of 8 rpm) and in discrete mode (with a stop for 20 seconds near each of the plasma sources or with a stop of 120 s and 300 s for Cu and Nb layers, respectively). The total coating time was 1.5 hours. The thickness of the coatings was about 12 μm.

The phase-structural state of the samples was studied by X-ray diffractometry using a DRON-4 apparatus in Cu-Kα radiation. To monochromatize the detected radiation, a graphite monochromator installed in the secondary beam (in front of the detector) was used. To decode the diffraction patterns, tables of the Powder Diffraction File international center were used [11]. The separation of profiles into components was carried out using the NewProfile software package (developed by NTU KhPI, Ukraine).

The surface morphology of the coated samples was studied using optical and scanning electron microscopy (SEM) on ZEISS AXIO Ver A1 instruments and FEI Nova NanoSEM 450, respectively.

The coatings were examined for their corrosion resistance during electrochemical processes. Electrochemical tests were carried out using a 3-electrode cell with a capacity of 200 ml and a Biologic SP-150 potentiostat. The cell consists of a coated sample (working electrode), a saturated calomel electrode (reference electrode), and a platinum electrode (counter electrode). Corrosion resistance was assessed by measuring the open-circuit potential for 1.5 hours in a solution of 0.9% NaCl at room temperature.

Impedance spectroscopy was performed in the frequency range from 10^{-2} to 10^{5} Hz. The potentiodynamic polarization test was carried out in the range from -0.6 to +1 V at a scan speed of 1 mV/s. The contact area of the sample with the electrolyte was 0.196 cm^2.

Determination of adhesive and cohesive strength, resistance to scratching and elucidation of the mechanism of destruction of coatings was carried out using a scratch tester Revetest (CSM Instruments). The contact load was 0.9 N, and the loading speed was 5 N/s.

3. Results and Discussion

The study of surface morphology showed that for coatings at a pressure of PN = $7 \cdot 10^{-4}$ Torr, the bias potential increases from -50V (Figure 1 a) to -100V (Figure 1 e) and - 200V (Figure 1 g) leads to a decrease in the number and size of the droplet phase. An increase in pressure from 7·10-4 to 3·10- 3 Torr (Figure 1 b) also leads to a decrease in the amount of the drop phase.

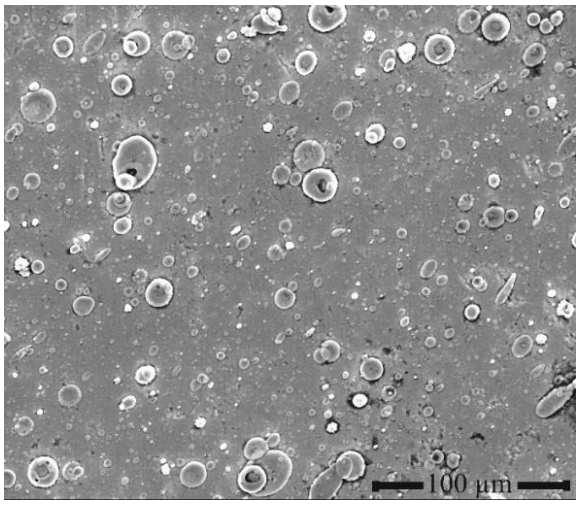

a

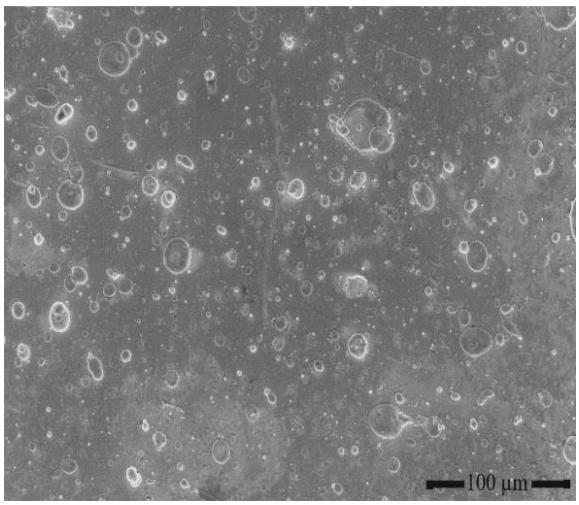

b

DOI: https://doi.org/10.30564/jmmr.v3i1.1364

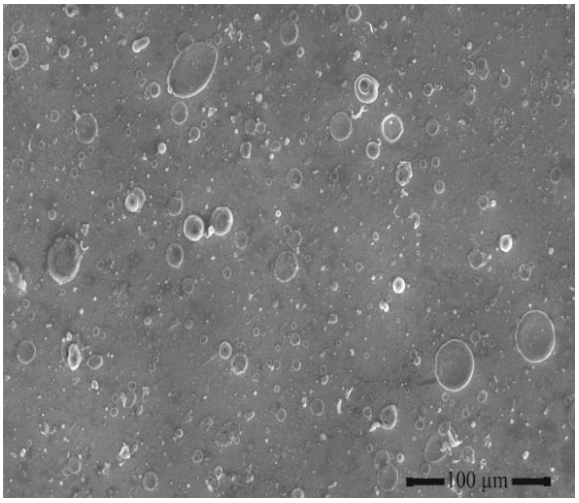

c

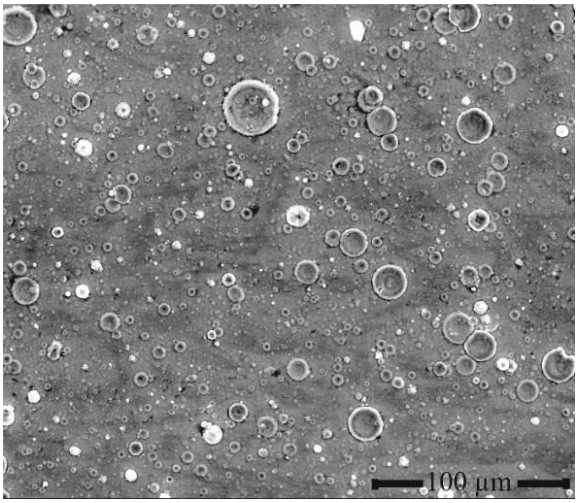

d

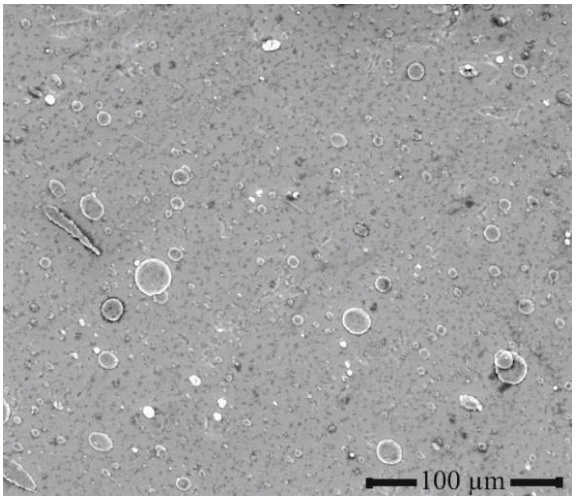

e

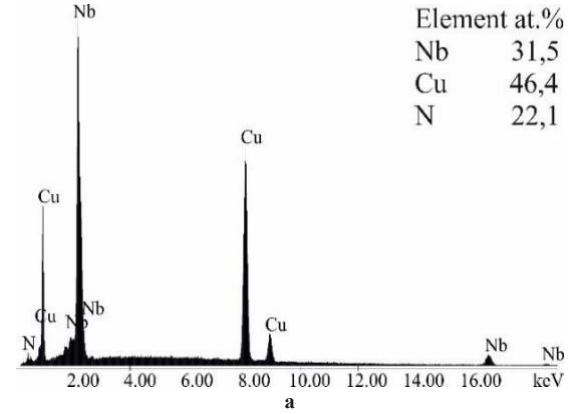

a

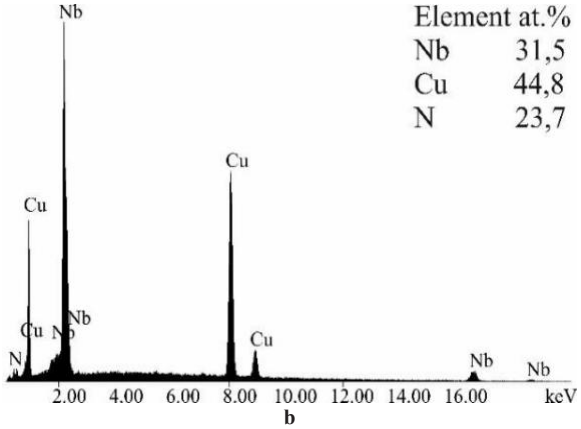

b

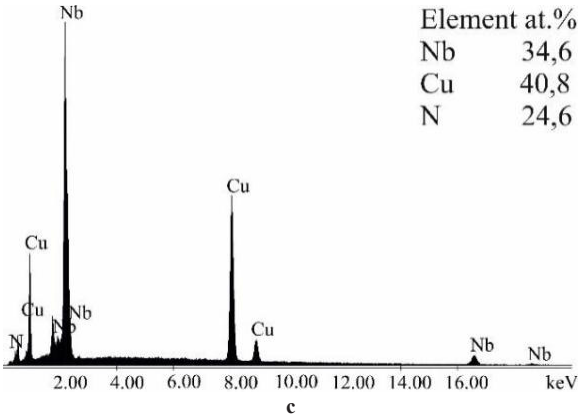

c

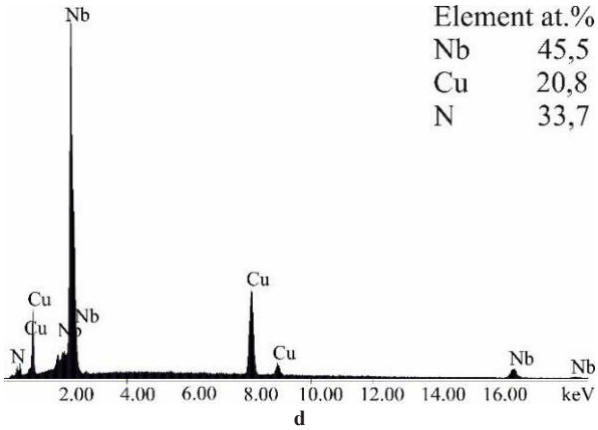

d

Figure 1. Surface morphology of coatings for the studied series of coatings

The energy dispersion spectra and elemental composition of the studied coatings are shown in Figure 2.

 DOI: https://doi.org/10.30564/jmmr.v3i1.1364

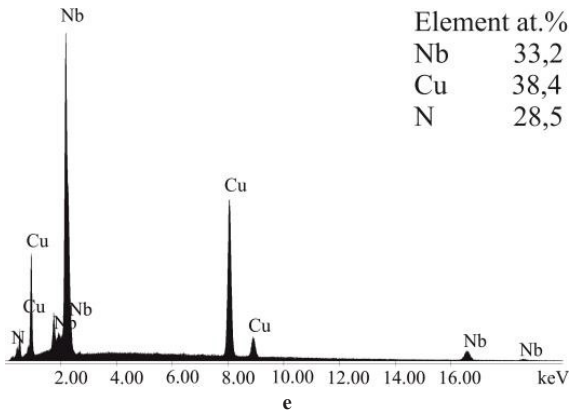

a - series 1, b - series 2, c - series 3, d - series 4, e - series 5

Figure 2. Energy dispersive spectra with data on elemental composition

It can be seen that for series 1 and 2 obtained in the constant rotation mode, the elemental composition remains almost unchanged with increasing pressure of the nitrogen atmosphere. Series 3 and 4, obtained at a pressure of PN = 7·10-4 Torr in the discrete mode, have a noticeable difference: with an increase in the bias potential from -50 V to -200 V, the amount of copper decreases by 2 times.

The study of the phase-structural state was carried out using the XRD method. The X-ray diffraction spectra of the coatings are shown in Figure 3.

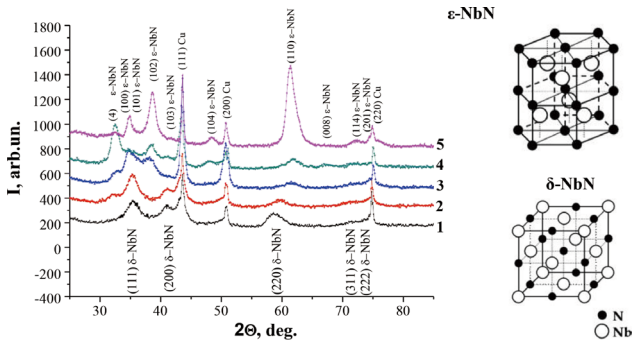

1 - PN = 7 · 10-4 Torr, Ub = -50 V; 2 - PN = 3 · 10-3 Torr, Ub = -50 V; 3 - PN = 7 · 10-4 Torr, Ub = -50 V; 4 - PN = 7 · 10-4 Torr, Ub = -200 V; 5 - PN = 3 · 10-3 Torr, Ub = -100 V

Figure 3. X-ray diffraction spectra of NbN/Cu multilayer coatings

It can be seen that at a relatively low pressure PN = $7 \cdot 10^{-4}$ Torr (spectrum 1, Figure 3) in the constant rotation mode, two phases are formed with an fcc crystal lattice (structural type NaCl): metastable δ-NbN (JCPDS 38-1155) and Cu (JCPDS 89-2838). The peak ratio is close to the standard for the fcc lattice; therefore, no pronounced texture is observed. An increase in pressure to 3·10-3 Torr (spectrum 2, Figure 3) leads to a qualitative change in diffraction spectra. In addition to the formation of the axis of preferential orientation [11], a diffraction peak is revealed from the equilibrium ε-NbN (JCPDS 89-4757) phase with a hexagonal lattice.

An increase in the layer thickness to 40 nm (spectra 3, 4, Figure 3) leads to the formation of only the equilibrium ε-NbN phase and Cu. An increase in the bias potential to Ub = –200 V (spectrum 4, Figure 3) does not lead to a change in the phase composition. However, in this case, the preferred orientation of crystallites with the (004) plane perpendicular to the growth surface is formed.

At the largest layer thickness (about 240 nm for Cu and 600 nm for NbN), a complete spectrum of diffraction peaks of ε-NbN and Cu phases is formed without a noticeable preferential orientation (spectrum 5, Figure 3).

Corrosion testing allowed us to determine the potential (Ecorr) and current (Icorr) of corrosion by extrapolation using the Tafel method. Figure 4 presents potentiodynamic polarization curves (graphs of the dependence of the potential on the density of the logarithm).

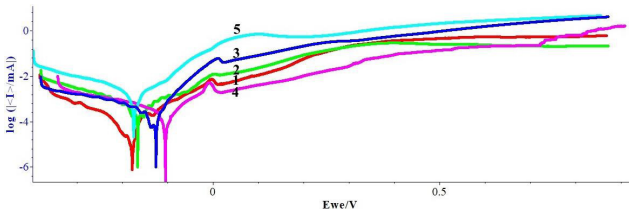

1 – series 1, 2 – series 2, 3 – series 3, 4 – series 4, 5 – series 5

Figure 4. Potentiodynamic polarization curves

As can be seen from Figure 4, for all series of coatings, the process is controlled by the anode part of the polarization curves [12]. From the above curves, the slope coefficients of the linear sections of the anode and cathode parts βc and βa were obtained (Table 2).

The corrosion rate is proportional to the corrosion current and was calculated by the formula

$$CR = \frac{I_{corr} \cdot K \cdot EW}{d \cdot A}, \quad (1)$$

where CR is the corrosion rate, mm/year; Icorr - corrosion current, mA; K is the conversion factor determining the unit of measurement of the corrosion rate; EW - equivalent weight, gram- equivalent; d is the density, g/cm^3; A is the sample area, cm^2.

Additionally, the polarization resistance (Rp) of the Tafel curves was calculated using the Stern-Geary equation [13], which takes into account both the current density and the slope of the polarization curves.

The calculation results are given in table 2.

DOI: https://doi.org/10.30564/jmmr.v3i1.1364

Table 2. Potentiodynamic polarization test results

Series	Ecorr, mV	Icorr, mA	βa, mV	βc, mV	CR, mm/year	Rp, Ohm·cm²
1	-208,347	$9 \cdot 10^{-5}$	119,2	103,6	$8{,}14 \cdot 10^{-3}$	5252,8
2	-138,302	$4{,}21 \cdot 10^{-4}$	104,2	187,5	$38 \cdot 10^{-3}$	13563,2
3	-258,219	$1{,}17 \cdot 10^{-3}$	181,7	290,0	$106 \cdot 10^{-3}$	8094,8
4	-303,715	$1{,}96 \cdot 10^{-3}$	2155,7	286,3	$176 \cdot 10^{-3}$	10976
5	-174,249	$1{,}48 \cdot 10^{-3}$	83,4	156,5	$134 \cdot 10^{-3}$	2352

As can be seen from the table 2, all coatings have good corrosion resistance, regardless of the coating conditions (table 1). However, the results show that the application mode and the number of layers change the resistance of the coating in an aggressive environment. So, the best indicators of corrosion resistance are characteristic of coatings of series 1 and 2 obtained in the continuous deposition mode (when the layer thickness is minimal and about 8 nm), as well as with the smallest bias potential (Ub = -50V). Which may be explained by the lower defectiveness of thin layers.

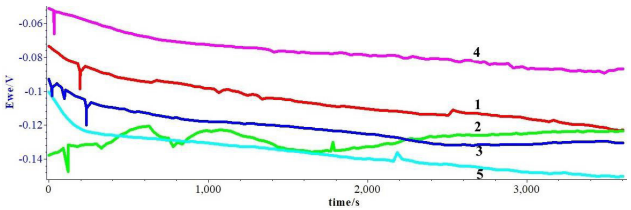

1 – series 1, 2 – series 2, 3 – series 3, 4 – series 4, 5 – series 5

Figure 5. Curves of corrosion potential over time

As can be seen from the curves in Figure 5, during the interaction of the coating with the electrolyte medium, the surface layer slowly dissolves with a slight manifestation of pitting. This situation is typical for the series of samples 1, 3, 4. To a greater extent, the same trend is observed for series 5 (except for pitting formation). The behaviour of the coating of series 2 is radically different. At the initial time, the corrosion potential is relatively large, but it decreases with a tendency to stabilize.

The resistance of charge transfer through protective coatings using Nyquist curves was also evaluated. The curves themselves for the systems under consideration and the equivalent circuit model are shown in Figure 6.

Based on the conducted corrosion tests, the best indicators of corrosion resistance were shown by coatings of series 1 and 2. Additionally, studies were carried out for these 2 series, which allow us to determine one of the most important characteristics of the mechanical properties of coatings - adhesive strength. To determine it, the method of scratch testing was used.

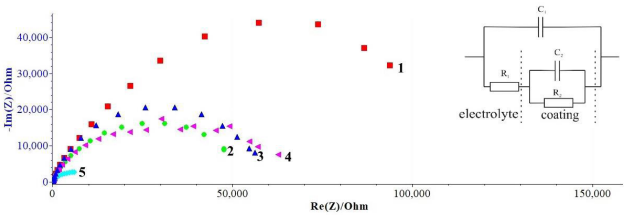

C1, C2 - the capacity of the double layer and coating, respectively; R1, R2 - resistance of the electrolyte and phases in the coating, respectively 1 – series 1, 2 – series 2, 3 – series 3, 4 – series 4, 5 – series 5

Figure 6. Nyquist curves and equivalent electrolyte-coating circuit model

Figure 7 shows the wear paths in the region of LC critical points during loading. The resulting critical point values for these areas are given in table 3.

LC1

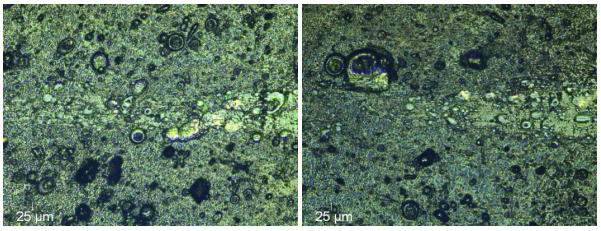

a **b**

LC2

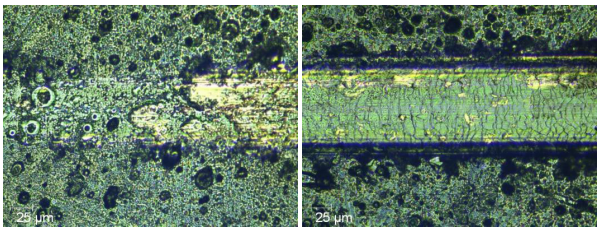

a **b**

LC3

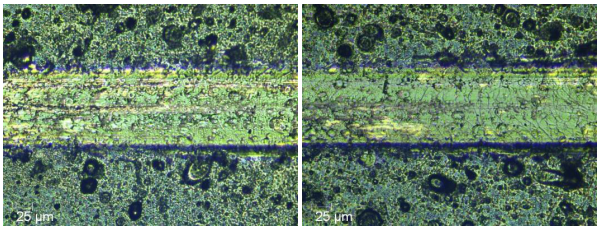

a **b**

LC4

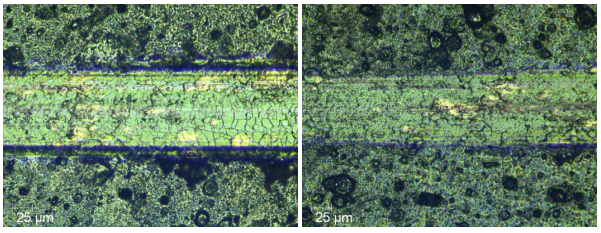

a **b**

Figure 7. Wear paths at critical points under LC loading for coatings of series 1 (a) and 2 (b)

 DOI: https://doi.org/10.30564/jmmr.v3i1.1364

Table 3. The magnitude of the load in the region of critical points LC

Series	The value of the load in the region of critical points, N				
	LC1	LC2	LC3	LC4	LC5
1	23.6	29.5	34.3	38.6	61.8
2	23.8	30.3	35.3	40.1	96.5

It can be seen that in the area of primary crack formation and up to the critical point LC4, coatings of series 1 and 2 have almost the same values. However, the critical point LC5 (the load at which complete abrasion of the coating occurs) is higher for series 2. This can be attributed to a change in the phase-structural state and the appearance of the ε-NbN phase, as well as a significant decrease in the droplet phase on the coating surface.

4. Conclusions

Studies have shown that the technological parameters of deposition have a significant impact on the phase-structural state, corrosion resistance and adhesive strength. An optimal deposition mode has been established to obtain the best corrosion resistance indicators: a bias potential of -50 V at the smallest layer thickness of ~ 8 nm. In this mode, a metastable phase of δ-NbN and Cu with a face-centered crystal lattice is formed. Comparison of coatings of series 1 and 2 (showing the best values of corrosion resistance) on adhesive strength show that higher adhesion strength indications for series 2 (critical load LC5 = 96.524 N). Based on the data obtained, it is clear that there is no universal structural state that provides both the highest adhesive strength and corrosion resistance. However, the necessary functional properties can be achieved by structural engineering at the stage of coating formation. In this work, it was found that the complex of the highest functional characteristics is characteristic of coatings of series 1. They were obtained at a pressure of 7·10-4 Torr, a bias potential of -50 V, a layer thickness of 8 nm and have a δ-NbN phase in niobium layers (no pronounced texture is observed). These coatings have the best indicators of corrosion resistance among the investigated series of coatings, while also quite high values of adhesive strength. The assessment showed that with a thickness of such a coating of about 10 microns, the resource of its operation in an aggressive environment is about a year.

Acknowledgments

The authors are grateful to prof. A.A. Andreev and PhD V.A. Stolbovoy for help in obtaining coatings.

References

[1] Volkov, A.I., Zharskiy, I.M. Bolshoy himicheskiy spravochnik[M]. Mn.: Sovremennaya shkola, 2005: 608.

[2] Guzmana, P., Caballeroa, J.L., Orozco-Hernándezb, G., Aperadora, W., Caicedoc, J.C. Tribocorrosion Behavior of Niobium-Based Thin Films for Biomedical Applications[J]. Tribology in Industry, 2018, 40(4): 624-632. DOI: 10.24874/ti.2018.40.04.09

[3] Ren, P., Wen, M., Du, S.X., Meng, Q.N., Zhang, K., Zheng, W.T. Microstructure, mechanical and tribological properties of NbN/Ni coatings[J]. Materials Science Forum, 2017, 898: 1424-1430. DOI: www.scientific.net/MSF.898.1424

[4] Courtney, T.H., Reintjes, J., Wulff, J. Critical Field Measurements of Superconducting Niobium Nitride[J]. J. Appl. Phys., 1965, 36: 660. DOI: 10.1063/1.1714056

[5] Lengauer, W., Bohn, M., Wollein, B., Lisak, K. Phase reactions in the Nb–N system below 1400°C[J]. Acta Materialia, 2000, 48(10): 2633-2638. DOI: 10.1016/S1359-6454(00)00056-2

[6] Sobol', O.V., Postelnyk, A.A., Meylekhov, A.A., Andreev, A.A., Stolbovoy, V.A., Gorban, V.F. Structural Engineering of the Multilayer Vacuum Arc Nitride Coatings Based on Ti, Cr, Mo and Zr[J]. Journal of nano- and electronik physics, 2017, 9(3): 03003. DOI: 10.21272/jnep.9(3).03003

[7] Sobol', O.V., Andreev, A.A., Gorban', V.F., Stolbovoy, V.A., Meylekhov, A.A., Postelnyk, A.A. Possibilities of structural engineering in multilayer vacuum-arc ZrN/CrN coatings by varying the nanolayer thickness and application of a bias potential[J]. Technical Physics, 2016, 61(7): 1060. DOI: 10.1134/s1063784216070252

[8] Musil, J., Zeman, P., Hruby', H., Mayrhofer, P.H. ZrN/Cu nanocomposite film—a novel superhard material [J]. Surface and Coatings Technology, 1999, 120–121: 179–183. DOI: 10.1016/S0257-8972(99)00482-X

[9] Musil, J. Hard and superhard nanocomposite coatings[J]. Surface and Coatings Technology, 2000, 125(1-3): 322-330. DOI: 10.1016/S0257-8972(99)00586-1

[10] Sobol, O.V., Andreev, A.A., Corban', V.F. Structural engineering of vacuum-arc multiperiod coatings[J]. Metal Science and Heat Treatment, 2016, 58(1-2): 37. DOI: 10.1007/s11041-016-9961-3

[11] http://www.icdd.com

[12] Ramoul, C., Beliardouh, N.E., Bahi, R., Nouveau, C., Abdelghani, D., Walock, A.: Surface performances of PVD ZrN coatings in biological environments[J]. Tribology – Materials, Surfaces & Interfaces, 2018, 13: 12-19. DOI: 10.1080/17515831.2018.1553820

[13] Shrayera, L.L. Korroziya[M]. Sprav. M.: Metallurgiyu, 1981: 632.

DOI: https://doi.org/10.30564/jmmr.v3i1.1364